Proc. Natl. Acad. Sci. USA
Vol. 88, pp. 53–57, January 1991
Neurobiology

Sequence and functional expression in *Xenopus* oocytes of a human insulinoma and islet potassium channel

(cDNA/gene/insulin secretion/Shaker/delayed rectifier)

LOUIS H. PHILIPSON*, RITA E. HICE*, KRISTEN SCHAEFER*, JOSEPH LAMENDOLA†, GRAEME I. BELL*†‡, DEBORAH J. NELSON*§¶, AND DONALD F. STEINER*†‡‖

Departments of *Medicine, †The Howard Hughes Medical Institute, ‡Departments of Biochemistry and Molecular Biology, §Neurology, and ¶the Committee on Cell Physiology, The University of Chicago, 5841 S. Maryland Ave., Box 23, Chicago, IL 60637

Contributed by Donald F. Steiner, September 5, 1990

ABSTRACT **Regulation of insulin secretion involves the coordinated control of ion channels in the β-cell membrane. We have isolated and characterized cDNA and genomic clones encoding a voltage-dependent K^+ channel isoform expressed in human islets and in a human insulinoma. This K^+ channel isoform, designated hPCN1, with a deduced amino acid sequence of 613 residues (M_r = 67,097), is related to the Shaker family of *Drosophila* K^+ channels. hPCN1 is homologous to two other human K^+ channel isoforms we have isolated, hPCN2 and hPCN3, with 55% and 65% amino acid sequence identity, respectively. The electrophysiological characteristics of hPCN1 were determined after microinjection of synthetic RNA into *Xenopus* oocytes. Two-microelectrode voltage-clamp recordings of oocytes injected with hPCN1 RNA revealed a voltage-dependent outward K^+ current that inactivated slowly with time. Outward currents were inhibited by 4-aminopyridine with a K_i less than 0.10 mM and were relatively insensitive to tetraethylammonium ion or Ba^{2+}. A delayed rectifier K^+ channel such as hPCN1 could restore the resting membrane potential of β cells after depolarization and thereby contribute to the regulation of insulin secretion.**

K^+ channels have been implicated in the regulation of the electrical activity of β cells in response to glucose as well as to the sulfonylurea oral hypoglycemic agents (1–6). The initial β-cell response to glucose metabolism or sulfonylureas is closure of ATP-sensitive K^+ channels. This results in depolarization of the membrane potential, thereby opening voltage-sensitive Na^+ and Ca^{2+} channels giving rise to action potentials. The resting membrane potential is then restored by K^+ channels, which open in response to both the change in membrane potential and Ca^{2+} influx (3–6). The time course of activation and inactivation of K^+ channels serves to entrain the frequency and modulate the duration of Ca^{2+}-dependent action potentials and thus regulate insulin release (3–6).

An extended family of four voltage-gated K^+ channel genes has been described in *Drosophila*: Shaker (*Sh*), Shab, Shaw, and Shal (7–11). Alternative splicing of the Shaker and Shab genes has been shown to be a mechanism for generating further channel diversity (10–12). By using homology screening, expression cloning, or the polymerase chain reaction (PCR), cDNAs and genes encoding a family of K^+ channels related to each of the *Drosophila* K^+ channel genes have been identified in mammalian tissues and cell lines (10–20). The data suggest that K^+ channel diversity in mammalian tissues is a consequence of the presence of multiple genes that lack introns and hence are not subject to alternative splicing as a mechanism for generating multiple isoforms (7, 17, 18, 23). Additional diversity may be achieved by formation of heteromultimers between the products of these different mammalian genes (21–23).

As a first step in characterizing the ion channels expressed in β cells, we screened a human insulinoma cDNA library for voltage-gated K^+ channels by low-stringency cross-hybridization with a probe encoding the highly conserved membrane-spanning S4–H5 region of a rat brain K^+ channel isoform (13). The cDNA clones obtained did not contain all of the protein coding region, and the remainder was determined by isolating and sequencing the gene, designated hPCN1** (see Fig. 1).

The hPCN1 gene is most closely related to the Shaker gene in *Drosophila*. Comparison of the sequences of hPCN1 and other K^+ channels suggests that hPCN1 may be the human homolog of a rat K^+ channel, the partial sequence of which was obtained by PCR of rat islet and rat insulinoma RNA (20); the complete sequence of this rat protein, kv1, was recently described (17). Amplification of hPCN1 mRNA in human islet RNA indicated that it is also present in this tissue. Expression of hPCN1 in *Xenopus* oocytes indicated that it has characteristics of delayed rectifier-type channels. The pharmacological properties of hPCN1 are similar to the rat brain K^+ channel kv1 (17) but are distinct from other mammalian K^+ channels.

MATERIALS AND METHODS

General Methods. Standard procedures were as described (24). A 263-base-pair (bp) probe, pKC6, was generated from rat brain RNA corresponding to nucleotides 874–1137 of the MBK1 (mouse brain K^+ channel) cDNA sequence (13) by PCR and was used to screen a human insulinoma cDNA library (25). One clone was identified, λhKC-1, under low-stringency conditions (26), and the insert from this clone was used to rescreen the cDNA library and a genomic library (27).

Amplification of hPCN1 mRNA in Human Tissues. To detect the presence of the specific hPCN1 transcript in a malignant human β-cell tumor (provided by K. M. Pinnamaneni, A. O'Connor, and B. D. Ragsdale, Mesa, AZ) and normal human islets (RNA provided by S. Seino, University of Chicago, Chicago, IL), oligonucleotide primers were designed to amplify the 3′ untranslated region in two steps. First-strand cDNA was primed with a $(dT)_{17}$-adapter as described (28, 29) and then amplified by using sense oligonucleotides from the H6 membrane-spanning region of

The publication costs of this article were defrayed in part by page charge payment. This article must therefore be hereby marked "*advertisement*" in accordance with 18 U.S.C. §1734 solely to indicate this fact.

Abbreviations: 4-AP, 4-aminopyridine; Et_4N^+, tetraethylammonium ion; PCR, polymerase chain reaction.

‖To whom reprint requests should be addressed.

**The nucleotide sequences for the deduced protein sequences reported in this paper have been deposited in the GenBank data base (accession nos. M55513 for hPCN1, M55514 for hPCN2, and M55515 for hPCN3) and are also available from the authors.

hPCN1 (see Fig. 1) (TGTGCCATCGCCGGGGTCCT) and the adapter in the antisense direction (29). An aliquot was removed and reamplified with an internal primer pair (sense, GCAGACTGGTGGCAGTGG; antisense, ACAGGAAACAGAACAGCC). Positive (hKC-1 cDNA) and negative (water) controls were run with each sample.

***Xenopus* Expression Vector.** *Bam*HI linkers were added to a *Sac* II/*Eco*RV genomic fragment encoding hPCN1 and ligated into the *Bgl* II cloning site of pSP64T (30). This plasmid was linearized with *Eco*RI or *Sal* I, and SP6 transcripts were prepared with kits from Promega and Stratagene. The transcripts include 89 bp of 5′ and 141 bp of 3′ untranslated regions of *Xenopus* β-globin mRNA as well as the hPCN1 sequence.

Oocyte Injection. Adult female *X. laevis* (Xenopus I, Ann Arbor, MI) were maintained, and oocytes were harvested by published methods (31). Defolliculated oocytes were microinjected with ≈50 nl of solution containing 0.1–2 ng of *in vitro* transcribed RNA or water and incubated at 19°C in OR-2 medium (31).

Current Recording and Data Analysis. Current recordings using a two-microelectrode voltage clamp were made with a commercially available amplifier (Warner Instruments, Hamden, CT) from oocytes 8 hr to 8 days after RNA injection. Microelectrodes filled with 3 M KCl had resistances of 0.3–0.6 MOhm. OR-2 medium without pyruvate or gentamicin was used as the standard recording solution. Current decays were analyzed as a sum of exponentials by a Fourier method (32) that determined the number, amplitudes, and time constants of the components. Where three or more experiments were performed, values were reported as either the mean ± SEM or as the range with the number of experiments in parentheses.

RESULTS

Isolation and Sequence of Human K^+ Channel Clones. Screening of a human insulinoma cDNA library by hybridization under low-stringency conditions with a 263-bp rat brain K^+ channel cDNA probe identified a single positive clone, λhKC-1, having a 1.8-kilobase (kb) *Eco*RI insert. The sequence of this clone revealed that it encoded part of a protein homologous to rodent brain K^+ channels (13). As the murine genes encoding K^+ channels expressed in brain do not contain introns (18), we isolated a human genomic clone, λhPCN1, to obtain the complete sequence of this human K^+ channel isoform, designated hPCN1. The insert in this genomic clone contained *Eco*RI fragments of 3, 4, and 9 kb; the 9-kb fragment hybridized to the insert from the cDNA clone λhKC-1. The composite sequence of hPCN1 was obtained from the sequences of the cDNA and genomic clones.

The hPCN1 sequence contains an open reading frame of 1839 bp that was predicted to encode a 613-amino acid protein (M_r = 67,097); there are translation termination codons in all three frames upstream of the predicted initiating ATG (33). The deduced amino acid sequence of hPCN1 has 50–87% identity and 65–93% similarity with previously described rodent K^+ channel isoforms. hPCN1 is also related to two other human K^+ channel isoforms we have recently characterized. The amino acid sequence identity between hPCN1 and hPCN2 is 55% and between hPCN1 and hPCN3 is 67% (Fig. 1). The sequences are highly conserved in the membrane-spanning domains (H1, H2, H3, S4, H4, H5, and H6), including the presence of the Shaker-type (Arg or Lys-Xaa-Xaa)$_7$ repeat in S4. A putative leucine zipper sequence is also conserved in the S4–H4 region (34). The amino terminus of hPCN1 is divergent from other members of the family until residue 121, just prior to the first putative N-linked glycosylation site [Asn-Xaa-(Ser or Thr)], which also is conserved in the Shaker and Shal families (10, 11, 13). A putative calcium/calmodulin protein kinase II phosphorylation site [Arg-Xaa-Xaa-(Ser or Thr)] is conserved in hPCN1 at threonine-133 as well as similar locations in Shaker, Shal, Shab, and Shaw (35). A consensus protein kinase A phosphorylation site [(Arg or Lys)-(Arg or Lys)-Xaa-(Xaa)-(Ser or Thr); refs. 36 and 37] at hPCN1 serine-557 is conserved in Shaker and Shab; a second such site is found at serine-580. An additional feature of hPCN1 is an almost perfect direct repeat from residues 61–82, which contains a proline-rich region with homology to a similar region in the recently reported rat brain K^+ channel RKShIIIA, related to the Shaw family (16).

hPCN1 most closely resembles the rat brain K^+ channel kv1 (17) among K^+ channel sequences described to date. The nucleotide sequence identity in the protein coding regions of hPCN1 and kv1 is 84%; the 5′ and 3′ untranslated regions are more divergent, having 71% and 69% identity, respectively. Amino acid sequence identity between these two proteins is 88%, with 94% similarity. While it is likely that kv1 is the rat

FIG. 1. Predicted amino acid sequences of three human K^+ channels. The human proteins are named P (potassium) CN (channel) 1, 2, and 3 by analogy to human sodium channels (hSCN). Cloning of hPCN1 is described in the text. The sequence of hPCN2 (45) was deduced from the sequence of a cDNA clone isolated from a human fetal skeletal muscle library. The sequence of hPCN3 was deduced from the sequence of a genomic clone obtained from the same genomic library as hPCN1 (ref. 27; L.H.P., J.L., and D.F.S., unpublished results). Amino acids are indicated by their single-letter abbreviations. Gaps introduced to generate this alignment are represented by periods. Potential membrane-spanning domains (13) are noted by dashed lines. Residues that are identical in the three human proteins are indicated by bold type.

isoform of hPCN1, there are several interesting sequence differences of possible function significance: two additional putative protein kinase A phosphorylation sites in kv1 and the absence of the direct repeat (hPCN1 residues 61–82) in kv1 (17). By PCR analysis of this region of the rat and human genes, we have confirmed that the repeat is present in the human gene but lacking in the rat (data not shown). In contrast, other human/rat homologous isoforms share greater amino acid sequence identity: 97% between hPCN2 and RCK4 and 97% between hPCN3 and RCK3 (Fig. 1) (14).

Tissue Distribution of PCN1 mRNA. Northern blotting with 10 μg of total RNA prepared from various adult human tissues and several solid tumor cell lines revealed hybridization to a single faint transcript of about 4 kb in a human insulinoma (different from those that were combined to construct the insulinoma cDNA library) (data not shown). The transcript was more clearly evident with 5 μg of poly(A)$^+$ RNA from this human insulinoma. Transcripts of similar size were also obtained from RIN 5FS and HIT m2.2 cell RNA (data not shown). No hybridization was seen to total cellular RNA from human brain, skeletal muscle, liver, kidney, skin fibroblasts, or HepG2 cells, indicating that if hPCN1 is expressed in these tissues, the abundance of its RNA is less than in the insulinoma. Using RNA amplification of the 3′ untranslated region, we have been able to show that hPCN1 RNA is also present in normal human islets (data not shown).

Expression of hPCN1 in *Xenopus laevis* Oocytes. K^+ channels expressed after injection of hPCN1 RNA into *Xenopus* oocytes were characterized by using a two-microelectrode voltage clamp. Outward currents in noninjected control oocytes were typically less than 250 nA during steps to +100 mV from a holding potential (V_h) of −80 mV (data not shown). Slowly inactivating outward K^+ currents were elicited by depolarizing voltage steps positive to −30 mV in RNA-injected oocytes (Fig. 2 *Upper left*). At the higher RNA concentrations used (≈2 ng per oocyte), outward currents greater than 1 μA were recorded at 8 or more hr after RNA injection (Fig. 2 *Lower left*).

The threshold for hPCN1 activation was −25 mV. The time course of current activation decreased with increasing depolarization and could be fit with two exponentials (Fig. 2 *Right*). The ratio of the amplitudes of the two time constants describing the activation process increased with increasing depolarization (in three experiments, $A_{\tau 1}/A_{\tau 2}$ was 2.18 ± 0.1 and 4.73 ± 0.40 at −10 and 60 mV, respectively). The mean time constant of current activation for the three cells in Fig. 2 *Right* was 8.33 ± 0.36 msec at 0 mV and 1.35 ± 0.06 msec at 60 mV. The activation kinetics of hPCN1 and kv1 appear similar when expressed in *Xenopus* oocytes.

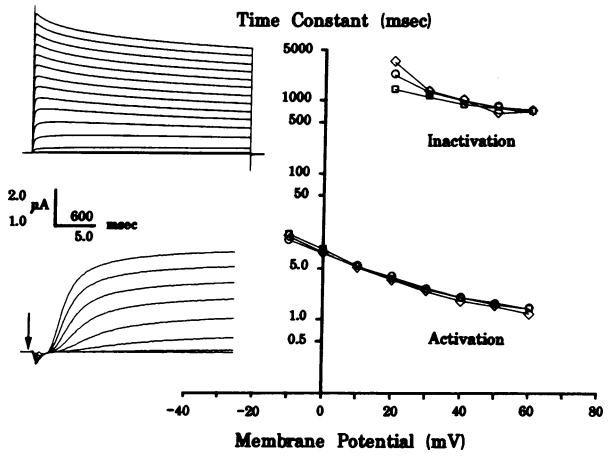

FIG. 2. (*Right*) Activation and inactivation time courses of hPCN1 K^+ currents (n = 3). Sampling rate/filter cutoff values were 5 kHz/2.5 kHz for activation and 2 kHz/1 kHz for inactivation. Current inactivation was fitted from peak current to the end of 1-sec depolarizations to the potentials indicated. (*Upper Left*) Currents obtained during 3.2-sec depolarizing steps from −70 to 60 mV in 10-mV increments; V_h = −80 mV. Currents are shown unsubtracted for leak or capacity transients. (*Lower Left*) Onset of currents evoked during steps from −30 to 40 mV in 10 mV increments in an oocyte 18 hr after RNA injection; V_h = −40 mV, subtracted with equal but opposite polarity steps. The arrow marks the start of depolarization; inward deflection is a subtraction artifact.

The expressed hPCN1 K^+ currents inactivated slowly with time during steps to positive voltages (Fig. 2 *Right*) most closely resembling RCK1 among the rat brain K^+ channels described by Stühmer and co-workers (14). The time constants of inactivation as determined from single exponential fits to the current data are plotted as a function of voltage in Fig. 2. Inactivation of the K^+ current was relatively voltage independent. The mean time constant of current inactivation for the three cells in Fig. 2 was 1155 ± 54 msec at 30 mV and 690 ± 17 msec at 60 mV.

Representative steady-state inactivation and conductance–voltage relationships of hPCN1 expressed in oocytes are given in Fig. 3. Steady-state inactivation of the hPCN1 currents became apparent at holding potentials more positive than −50 mV, and the delayed outward currents were completely blocked by holding potentials more positive than −10 mV. For eight oocytes the mean midpoint of the steady-state inactivation curve obtained from similar fits to the data was −25.3 ± 0.4 mV with a slope factor of 3.5 ± 0.2 mV. At depolarizations greater than 30 mV, the current–voltage relationship for hPCN1 expressed in *Xenopus* oocytes was linear. The conductance–voltage relationship was determined from deactivating steady-state currents at −40 mV (Fig. 3). An envelope of tails (data not shown) was constructed to confirm the validity of this method (38, 39). Half-maximal current activation, $V_{1/2}$, was −6.0 ± 0.6 mV with a slope (k) of −6.4 ± 0.5 mV (n = 5).

The selectivity of the current was determined from tail-current experiments in which the K^+ concentration in the external solution was varied between 2.5 and 75 mM (Fig. 4, *A* and *B*). Tail currents reversed polarity at −35 mV and −4 mV with external K^+ concentrations of 25 (n = 5) and 75 mM (n = 2), respectively (Fig. 4*A*). The 31-mV shift in reversal potential was close to the expected shift of 28 mV for a K^+ selective current (Fig. 4*B*).

The pharmacology of the hPCN1 currents expressed in *Xenopus* oocytes was examined by using K^+ channel blockers 4-aminopyridine (4-AP), tetraethylammonium ion (Et_4N^+), and Ba^{2+}. hPCN1 K^+ currents were blocked by 4-AP (Fig. 4*C*); however, the block was dependent on current activation and enhanced by repetitive stimulation. Repetitive stimulation in the presence of 50 μM 4-AP resulted in 30–38% block of the outward current (n = 6) and 54–62% block with 100 μM 4-AP (n = 5). Outward currents remaining in the presence of 10 mM 4-AP were comparable to endogenous current levels (n = 3). The presence of 20 mM Et_4N^+ in the external medium had no significant effect on hPCN1 currents (n = 2). In comparison, both RCK1 (14) and kv1 are blocked by low concentrations of 4-AP [K_i = 1.0 mM and K_i < 0.5 mM, respectively (hPCN1 K_i < 0.1 mM)] but differ in their sensitivity to Et_4N^+ [K_i = 0.6 mM for RCK1 (14) versus K_i > 40 mM for kv1 (17) (hPCN1 K_i > 20 mM)]. Ba^{2+} (10 mM) partially blocked hPCN1 currents. Currents measured 25 msec after onset of steps to 40 mV were reduced by 53% (n = 2), and the percentage block decreased during the voltage step (Fig. 4*D*). No shift was observed in the current–voltage relationship in medium containing 10 mM Mg^{2+}. Increasing Ca^{2+} from 1 to 10 mM in the external solution, substitution of Mg^{2+} for Ca^{2+}, or addition of 100 μM Cd^{2+} to the external medium had no effect on hPCN1 currents.

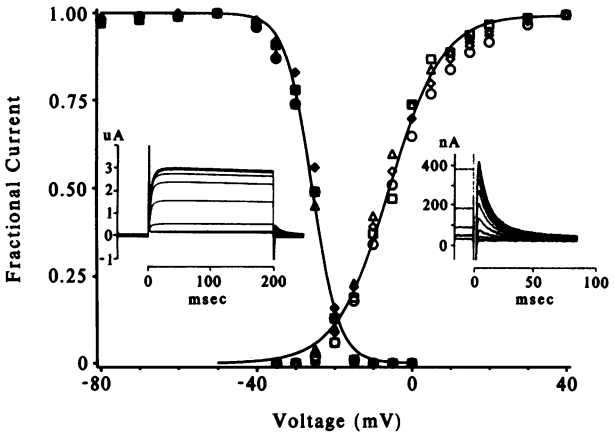

FIG. 3. Steady-state inactivation and conductance–voltage relationships. Steady-state inactivation (filled symbols) of hKCl currents in four oocytes is shown as a function of membrane potential. The steady-state parameters of activation and inactivation, $V_{1/2}$, k and $g_{K,max}$, were determined from conductance–voltage and steady-state inactivation curves fitted with a single Boltzmann isotherm of the form:

$$g_{K,(V)} = g_{K,max}/\{1 + \exp\{(V - V_{1/2})/k\}\}, \quad [1]$$

where $V_{1/2}$ is the voltage at the midpoint of the activation or inactivation curve and k is the steepness of the voltage dependence. A solid line represents the fitted curve (n = 4); the $V_{1/2}$ (−25.6 mV) and k (3.41 mV) values for the single curve were not significantly different from the fitted curves for each cell. The holding potential was varied from −80 to 0 mV (10-mV increments from −80 to −40 mV, 5-mV increments thereafter) for a period of 1 min prior to recording the K^+ current at a constant test potential of 40 mV. Currents elicited from holding potentials of −10, −5, and 0 mV showed no kinetic component and were averaged for subtraction from peak currents evoked from more negative holding potentials. (*Left Inset*) Effect of holding potential on currents elicited in one oocyte with the voltage protocol described. The conductance versus voltage relationships (open symbols) are shown for a second set of oocytes (n = 4). Conductance (g) was measured from deactivating steady-state currents using exponential fits to determine the amplitude of the instantaneous K^+ tail current. Conductances were normalized according to the relationship

$$g = I_{K,tail}/I_{K,tail,max}, \quad [2]$$

where $I_{K,tail,max}$ is the amplitude of the instantaneous current following a depolarization to 40 mV. The solid line represents the fitted curve for the four cells; the slope (−6.9) and midpoint (−5.7) for the single curve were not significantly different from the fitted curves for each cell. (*Right Inset*) Deactivating outward currents following depolarizing steps from −35 to 20 mV in 5-mV increments and steps to 30 and 40 mV. Outward currents during the activating steps are shown truncated and off scale. Instantaneous tail-current amplitudes were normalized to the value obtained following depolarizations to 40 mV.

DISCUSSION

In our initial studies of β-cell ion channels, we have characterized a K^+ channel, hPCN1, isolated from a human insulinoma cDNA library. The sequence of hPCN1 shows that it is related to the Shaker family of *Drosophila* K^+ channel genes. It is most similar to the rat brain K^+ channel isoform kv1 (17) but differs primarily by the presence of a proline-rich direct repeat in the amino-terminal cytoplasmic domain. RNA amplification by PCR has demonstrated the presence of hPCN1 RNA in normal human islets, suggesting that this K^+ channel may also participate in normal islet function. Expression of hPCN1 in *Xenopus* oocytes indicates that it is a K^+ channel with delayed rectifier kinetics.

Overexpression of a delayed rectifier such as hPCN1 would cause stabilization of the membrane resting potential. The presence of high levels of hPCN1 RNA in a malignant

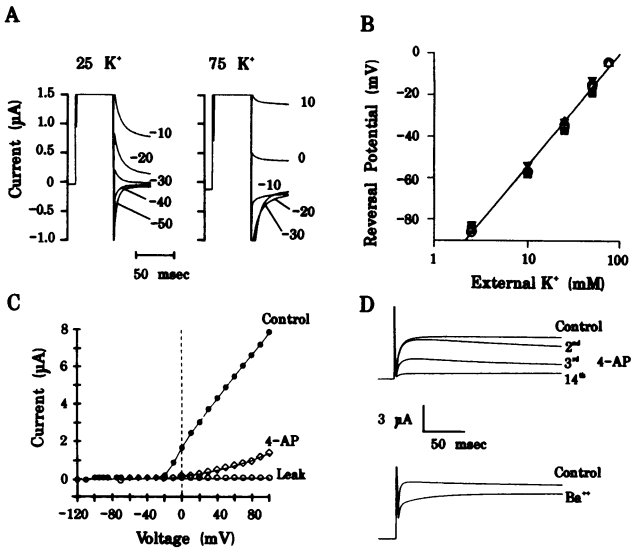

FIG. 4. Selectivity and pharmacology of hPCN1 K^+ currents. (*A*) Tail current reversal potentials shown for an oocyte in medium containing 25 mM and 75 mM K^+. Outward currents during the prepulses to 40 mV are shown. Test potentials are indicated for each tail current shown. (*B*) Plot of tail-current reversal potentials versus external K^+ concentration. Data are shown for five oocytes. The line through the data points represents the linear least-squares regression fit to the logarithmic transform of the data and has a slope of 54 mV per decade in external K^+ concentration. (*C*) Current–voltage relationship for an oocyte in OR-2 medium (control, ●) and in 1 mM 4-AP (◇); V_h = −80 mV. Current–voltage relationship in 4-AP was obtained after repetitive stimulation to maximize the 4-AP block (see *D*). Current values plotted are not leak-subtracted. Leakage current in OR-2 medium estimated from steps from −70 to −40 mV is also shown (○). Currents during hypolarizing steps are shown only for OR-2. (*D*) Block of hPCN1 K^+ currents by 4-AP and Ba^{2+}. (*D Upper*) Records showing the onset of block of 4-AP (1 mM) with the same cell as in *C*. The uppermost trace shows the current evoked during the step to 40 mV in OR-2 (control). The lower three traces are the second, third, and fourteenth step to 40 mV after addition of 1 mM 4-AP to the bath. The apparent shift in kinetics during steps 2 and 3 is due to use-dependence of the 4-AP block. The interpulse interval was 15 sec. (*D Lower*) Records showing currents evoked in OR-2 medium (control) and in 10 mM Ba^{2+}-containing medium during steps to 100 mV; V_h = −80 mV for both records.

human insulinoma may therefore account for the reduced glucose-responsiveness of insulin secretion in some insulinomas as compared with normal β cells (40). This expression in some tumors may also reflect differences in gene regulation between fetal and adult islets. Fetal β cells secrete insulin poorly in response to glucose (41–43). Cell-attached patch recordings of these cells are dominated by a small conductance K^+ channel, consistent with a delayed rectifier (43). K^+ currents through channels of this type could stabilize the membrane potential of fetal β cells below the threshold required for action potential initiation. Thus, the cells could remain quiescent even upon glucose-induced closure of the ATP-sensitive K^+ channels. This would explain the failure of tolbutamide, a sulfonylurea, to induce action potentials in the majority of such cells (43). Although alternative mechanisms have been proposed (40, 43), the possibility thus exists that both fetal β cells and some insulinomas are less responsive to glucose-induced insulin release than normal β cells in part because of increased expression of voltage-sensitive K^+ channels.

Voltage-sensitive K^+ channels in normal islets are critical in the restoration of the cell membrane to a hyperpolarized state after a calcium action potential (3, 5, 6, 44). The mouse β-cell voltage-sensitive K^+ channel was found to be sensitive to 4-AP and Et_4N^+ (3, 5); hPCN1 was sensitive to 4-AP but

resistant to Et_4N^+. However, the delayed rectifier currents seen in β cells may actually be produced by heteromultimeric K^+ channels, as RNA amplification of *ob/ob* mouse islets and rat and hamster insulinomas indicates that two to six different K^+ channel genes may be expressed in these cells (ref. 20; L.H.P. and D.F.S., unpublished results). Furthermore, when two rat K^+ channel isoforms with differing Et_4N^+ sensitivities were coexpressed in *Xenopus* oocytes, the Et_4N^+ sensitivity of the resulting current was intermediate to that of either isoform expressed alone (22, 23). Therefore, hPCN1 could play an important role in regulating membrane potential and the secretion of insulin in normal islets.

We thank C. Beck, C. Burant, J. Buse, S. Chan, J. Paul, J. Satin, S. Seino, T. Shapiro, S. Smeekens, and J. Whittaker for helpful discussions and P. Gardner for expert technical assistance. This work was supported by the Northern Illinois Section of the American Diabetes Association, The Howard Hughes Medical Institute, National Institutes of Health Grant RO1 GM36823 to D.J.N., the Diabetes Research and Training Center at the University of Chicago, National Institutes of Health Grants DK 13914 and DK 20595 to D.F.S. and P32 HL07381 to R.E.H., and a Juvenile Diabetes Foundation International Postdoctoral Fellowship to L.H.P.

1. Peterson, O. H. & Findlay, I. (1987) *Physiol. Rev.* **67,** 1054–1116.
2. Ashcroft, F. M. (1988) *Annu. Rev. Neurosci.* **11,** 97–118.
3. Satin, L. S., Hopkins, W. F., Fatherazi, S. & Cook, D. L. (1989) *J. Membr. Biol.* **112,** 213–222.
4. Boyd, A. E. (1988) *Diabetes* **37,** 847–50.
5. Bokvist, K., Rorsman, P. & Smith, P. A. (1990) *J. Physiol.* **423,** 311–325.
6. Smith, P. A., Bokvist, K., Arkhammar, P., Berggren, P. O. & Rorsman, P. (1990) *J. Gen. Physiol.* **95,** 1041–1059.
7. Baumann, A., Krah-Jentgens, I., Muller, R., Muller-Holtkamp, F., Seidel, R., Kecskemethy, N., Casal, J., Ferrus, A. & Pongs, O. (1987) *EMBO J.* **6,** 3419–3429.
8. Papazian, D. M., Scwarz, T. L., Tempel, B., Jan, Y. N. & Jan, L. Y. (1987) *Science* **237,** 749–753.
9. Kamb, A., Iverson, L. & Tanouye, M. A. (1987) *Cell* **50,** 405–413.
10. Butler, A., Wei, A., Baker, K. & Salkoff, L. (1989) *Science* **243,** 943–947.
11. Wei, A., Covarrubias, M., Butler, A., Baker, K., Pak, M. & Salkoff, L. (1990) *Science* **248,** 599–603.
12. Schwarz, T. L., Tempel, B., Papazian, D. M., Jan, Y. N. & Jan, L. Y. (1988) *Nature (London)* **331,** 137–142.
13. Tempel, B., Jan, Y. N. & Jan, L. Y. (1988) *Nature (London)* **332,** 837–839.
14. Stühmer, W., Ruppersberg, J. P., Schroter, K. H., Sakmann, B., Stocker, M., Giese, K. P., Perschke, A., Baumann, A. & Pongs, O. (1989) *EMBO J.* **8,** 3235–3244.
15. Frech, G. C., VanDongen, A. M., Schuster, G., Brown, A. M. & Joho, P. (1989) *Nature (London)* **340,** 642–645.
16. McCormack, T., Vega-Saenz de Miera, E. C., Rudy, B. (1990) *Proc. Natl. Acad. Sci. USA* **87,** 5227–5231.
17. Swanson, R., Marshall, J., Smith, J. S., Williams, J. B., Boyle, M. B., Folander, K., Luneau, C. J., Antanavage, J., Olivia, C., Buhrow, S. A., Bennet, C., Stein, R. B. & Kaczmarek, L. K. (1990) *Neuron* **4,** 929–939.
18. Chandy, K. G., Williams, C. B., Spencer, R. H., Aguilar, B. A., Ghanshani, S., Tempel, B. L. & Gutman, G. A. (1990) *Science* **247,** 973–975.
19. Kamb, A., Weir, M., Rudy, B., Varmus, H. & Kenyon, C. (1989) *Proc. Natl. Acad. Sci. USA* **86,** 4372–4376.
20. Betsholtz, C., Baumann, A., Kenna, S., Ashcroft, F. M., Ashcroft, S. J. H., Berggren, P., Grupe, A., Pongs, O., Rorsman, P., Sandblom, J. & Welsh, M. (1990) *FEBS Lett.* **263,** 121–126.
21. Isacoff, E. Y., Jan, Y. N. & Jan, L. Y. (1990) *Nature (London)* **345,** 530–534.
22. Ruppersberg, J. P., Schroter, K. H., Sakmann, B., Stocker, M., Sewing, S. & Pongs, O. (1990) *Nature (London)* **345,** 535–537.
23. Christie, M. J., North, P. A., Osborne, P. B., Douglass, J. & Adelman, J. P. (1990) *Neuron* **2,** 405–411.
24. Maniatis, T., Fritsch, E. F. & Sambrook, J. (1982) *Molecular Cloning: A Laboratory Manual* (Cold Spring Harbor Lab., Cold Spring Harbor, NY).
25. Sanke, T., Bell, G. I., Sample, C., Rubenstein, A. H. & Steiner, D. F. (1988) *J. Biol. Chem.* **263,** 17243–17246.
26. Kayano, T., Fukumoto, H., Eddy, R. L., Fan, Y.-S., Byers, M. G., Shows, T. B. & Bell, G. I. (1988) *J. Biol. Chem.* **263,** 15245–15248.
27. Lawn, R. M., Fritsch, E. F., Parker, R. C., Blake, G. & Maniatis, T. (1978) *Cell* **15,** 1157–1174.
28. Saiki, R. K., Scharf, S., Faloona, F., Mullis, K. B., Horn, G. T., Erlich, H. A. & Arnheim, N. (1985) *Science* **230,** 1350–1354.
29. Frohman, M. A., Dush, M. K. & Martin, G. R. (1988) *Proc. Natl. Acad. Sci. USA* **85,** 8998–9002.
30. Krieg, P. A. & Melton, D. A. (1987) *Proc. Natl. Acad. Sci. USA* **84,** 2331–2335.
31. Marcus-Sekura, C. J. & Hitchcock, M. J. M. (1987) *Methods Enzymol.* **152,** 284–287.
32. Provencher, S. W. (1976) *Biophys. J.* **16,** 21–41.
33. Kozak, M. (1989) *J. Cell Biol.* **108,** 229–241.
34. McCormack, K., Campanelli, J. T., Ramaswami, M., Mathew, M. K., Tanouye, M. A., Iverson, L. E. & Bernardo, R. (1989) *Nature (London)* **340,** 103.
35. Blackshear, P. J., Nairn, A. C. & Kuo, J. F. (1988) *FASEB J.* **2,** 2957–2962.
36. Glass, D. B. & Krebs, E. G. (1982) *J. Biol. Chem.* **262,** 772–775.
37. House, C. & Kemp, B. E. (1987) *Science* **238,** 1726–1728.
38. Giles, W. R. & Shibata, E. F. (1985) *J. Physiol.* **368,** 265–292.
39. Hodgkin, A. L. & Huxley, A. F. (1952) *J. Physiol.* **116,** 473–496.
40. Flatt, P. R. (1990) *Biochem. Soc. Trans.* **18,** 124–127.
41. Espinosa, M. M. A., Driscoll, S. G. & Steinke, J. (1970) *Science* **168,** 1111–1112.
42. Asplund, K. & Freinkel, N. (1978) *Diabetes* **27,** 611–619.
43. Rorsman, P., Arkhammar, P., Bokvist, K., Hellerstrom, C., Nilsson, T., Welsh, M., Welsh, N. & Berggren, P. (1989) *Proc. Natl. Acad. Sci. USA* **86,** 4505–4509.
44. Bokvist, K., Rorsman, P. & Smith, P. A. (1900b) *J. Physiol.* **423,** 327–342.
45. Philipson, L. H., Schaefer, K., LaMendola, J., Bell, G. I. & Steiner, D. F. *Nucleic Acids Res.*, in press.